Egypt. J. Chem. **Vol. 66,** No. 8 pp. 73 - 84 (2023)

Egyptian Journal of Chemistry

http://ejchem.journals.ekb.eg/

Studies on the uranium removal from aqueous solution of contaminated soil using natural zeolite

Ahmed S. Abd-Elaziz[1], El Sayed A. Haggag[1], Khaled G. Soliman[2], Mohammed S. Atress[1]

[1] *Nuclear Materials Authority, P.O. Box 530 Maadi, Egypt.*

[2] *Soil Sci. Dept., Fac of Agric., Zagazig University.*

Abstract

Zeolite as a low-cost adsorbent for the removal of uranium (VI) ions from aqueous solution under the effect of various process parameters such as the pH of the intermediate, contact time, adsorption temperature, initial uranium concentration and S/L ratio. The equilibrium and kinetic characteristics of the Zeolite from acidic medium have been determined. The purpose of this investigation was to evaluate adsorption of uranium (VI) from soil pre-contaminated with them as well as their removal using different solutions. Citric, Maleic, Succinic, Tartaric, Lactic and oxalic organic weak acids were used for removal of metals from soil by washing. The soil samples were collected from the surface layer (0 – 30 cm) in field of Inchass area, Sharkia governorate, Egypt. Soils were pre-contaminated with 100 ppm uranium citrate. Experiment involved the application of the weak organic acids in amounts of 0.5 - 3.0% to evaluate the leaching efficiency for the uranium. The practical adsorption capacity of uranium upon the resin under the optimum conditions has been found to attain 32 mg/g which matches with Langmuir isotherm 35 mg/g. The physical parameters including the adsorption kinetics, the isotherm models and the thermodynamic data have also been determined to describe the nature of the uranium adsorption by the natural zeolite. The working natural clinoptilolite found to agree with both the pseudo second order reaction and the Langmuir isotherm.

Keywords: Uranium removal, leaching agent, natural zeolite, adsorption isotherms.

1. Introduction

Uranium is one of the most serious contamination concerns because of its radioactivity and heavy-metal toxicity. Uranium and its compounds are highly toxic, which is a threat to human health and ecological balance**.** Many processes have been proposed for U(VI) ion removal from industrial wastewaters and radioactive wastes, with chemical precipitation, ion-exchange, membrane processes, solvent extraction and adsorption being the most commonly used methods employed [1–6]. Natural zeolite, as aluminosilicate mineral, has characteristics of large surface area, strong capability of ions exchange and adsorption for their particular tetrahedral pore framework. Moreover, they are one of low-cost and easily obtaining materials which have been used as an adsorption for removal of heavy metals [7–13]. Zeolite with framework structures is an excellent inorganic ion exchanger, having high stability constants and resistance to irradiation damage. Some zeolite has been used for processing of radioactive liquid wastes, owing to the strong affinity for toxic and problematic elements [14] and selectivity for some radionuclides [15]. Kilincarslan et al. [16] studied uranium adsorption characteristic and thermodynamic behavior of clinoptilolite zeolite. Misaelides et al. [17] studied uranium and thorium uptake by natural zeolitic materials. Krestou et al. [18] investigated the mechanism of aqueous U(VI) uptake by natural zeolitic tuff. Akyil et al. [19] also studied the distribution of uranium on zeolite and investigation of thermodynamic parameters for the uptake system. The use of natural materials including a clinoptilolite-bearing rock for the uptake of uranium from aqueous solutions in the presence of NaCl or $NaHCO_3$was also investigated by Ames et al. [20].The purpose of the present study was to test the properties of zeolite as an adsorbent for removing U(VI) ions from synthetic solutions. The effects of several variables, such as the initial U(VI) ion concentration, the initial pH and the presence of salt on the adsorption of U(VI) ions were investigated. The present work aims to evaluate the

Corresponding author e-mail smatreessemida@gmail.com.; (Mohammed S. Atress).

Received date: 27 June 2022; revised date: 20 September 2022; accepted date: 27 November 2022

DOI: 10.21608/ejchem.2022.147389.6390

©2023 National Information and Documentation Center (NIDOC

ability of some weak organic acids for leaching uranium from soil pre-contaminated as well as to evaluate the ability of different organic acids for leach uranium from pre-polluted soils.

2. Materials and Methods

2.1. Soils

Soils used in the experiments were collected from the surface layers (0 – 30 cm) of a field in Inchass area, Sharkia governorate, Egypt. The soil was a sandy loam where it was taken from field under arable cultivated and irrigated by sewage water for about 80 years. Some physical and chemical characteristics of this soil are shown in Table 1.

2.2. Leaching of contaminated soil

Water acidified with phosphoric acid until pH 2 or water was used for soil leaching test. Also, sex organic acids namely; lactic, tartaric, succinic, maleic, oxalic and citric acids, were used for soil washing test.

2.3. Chemicals and reagents

All chemicals used for analysis were analytical grade reagents. Uranyl sulfate trihydrate $UO_2SO_4.3H_2O$ from IBI labs, Florida, USA and HCl 37%, HNO_3, NaCl**.**

2.4. Preparation of the pregnant solutions:

- Generally, the samples used in this work were weighed using an analytical balance produced by Shimadzu (AY 220).
- Hot plate magnetic stirrer model Fisher Scientific.
- The hydrogen ion concentration of the different solutions was measured accurately using the pH- meter model (HAANA pH-mV-temp).
- The quantitative analysis of uranium was carried out by UV-spectrophotometer "single beam multi-cells-positions model SP-8001", Metretech Inc., version 1.02 using Arsenazo III indicator (Sigma-Aldrich) and confirmed by an oxidimetric titration against ammonium metavanadate using N-phenyl anthranilic acid indicator (Sigma-Aldrich) [21].

2.5. Experimental procedure:

The batch procedure was performed to optimize the basic equilibrium conditions for uranium adsorption such as pH, contact time, temperature and natural clinoptilolite to liquid ratio. In these experiments, 10 ml of 100 mg U/L solution were stirred with 0.05 g dry natural clinoptilolite 250 rpm in a 100 ml conical flask. After mixing the zeolite with the liquor, the two phases were decanted and the clear raffinate was analyzed against the uranium concentration. The amount of uranium adsorption q_e (mg/g) was calculated from the difference of uranium concentration in the aqueous solution before and after adsorption at the equilibrium time t according to equation (1):

$$q_e = (C_0 - C_e)\frac{V}{m} \qquad (1)$$

where Co and Ce are the initial and equilibrium concentrations of U (VI) in the solution (mol. L^{-1}), V is the volume of solution (L), m is the weight of the zeolite (g). The amount of U (VI) adsorbed onto the resin (q, mg/g) and the uptake percent (U %) were determined using equation (2).

$$U\,\% = \frac{(C_0 - C_e)}{C_e} \times 100 \qquad (2)$$

The distribution coefficient (K_d) of uranium between the aqueous bulk phase and the solid phase clinoptilolite was calculated from the following equation (3):

$$K_d = \frac{C_o - C_e}{C_e} \times \frac{V}{m} \qquad (3)$$

2.6. Optimization of the leaching process:

Due to the large number of mineral constituents in the study ore material, it was determined that the leaching potentialities of these essential metal values needed to be investigated.

2.7. Effect of parameters:

The results obtained from dissolution of contaminated soil with citric acid solution are discussed in the following section. The effects of reaction time, citric acid concentration, solid/liquid ratio, and temperature on the dissolution process were investigated in this study.

3. Results and Discussion

3.1. Effect of parameters:

The results obtained from dissolution of contaminated soil with citric acid solution are discussed in the following section. The effects of reaction time, citric acid concentration, solid/liquid ratio, and temperature on the dissolution process were investigated in this study.

3.1.1. Effect of organic acids types:

The effect of different organic acid types on U leaching from contaminated soil was investigated using fixed parameters such as 1.0 M organic acid type concentration, particle size 63µm, room temperature, stirring speed 600 rpm, stirring time 120 min, and S/L mass ratio: 1:10 g / ml. The experimental results shown in Fig (1) between U leaching efficiency and organic acid type show that, depending on the type of organic acid, the leaching percent of U is affected as

follows: lactic acid (20.4 % U) maleic acid (32.6 % U), succinic acid (22.9 % U), tartaric acid (53.3 % U), citric (82.3 % U) and oxalic acid (44.6 % U). As a result, citric acid is the acid of choice for the dissolution of contaminated soil in other experiments [22].

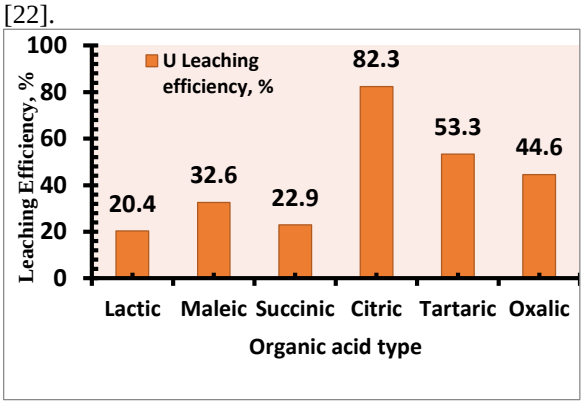

Fig. (1): Effect of organic acid types on U dissolution efficiency, % temperature: 25±1°C; particle size: 63 µm; [Organic acid]: 1.0 M; stirring time: 120 min; S/L mass ratio: 1:10 g / ml; stirring speed: 600 rpm).

3.1.2. Effect of Citric Acid Concentration:

Citric acid concentration ranging from 0.2 to 1.4 M affected the dissolution efficiency of U from contaminated soil was studied using solid / liquid ratio 1:10 g/ ml at room temperature with stirring speed of 600 rpm and 63 µm particle size. The results showed in Fig (2) as a relation between U leaching efficiency and citric acid concentration investigated that, the citric acid concentration increases from 0.2 to 1.0 M the U leaching efficiency raised from 24.0 to 82.3%. This may be due to the increase of the H+ ions in the solution. Further increase in citric acid concentration has a slight effect on U leaching percentage. Therefore, 1.0 M tartaric acid is preferred acid concentration used for the other experiments of the dissolution of the working sample [23].

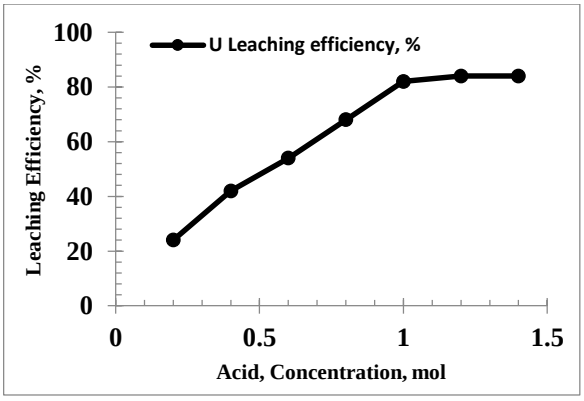

Fig. (2): Effect of citric acid concentration on U dissolution efficiency, % temperature: 25±1°C; particle size: 63 µm; stirring time: 120 min; S/L mass ratio: 1:10 g / ml; stirring speed: 600 rpm).

3.1.3. Effect of reaction time

This factor was investigated using a time range of 15 to 240 min at 600 rpm stirring rate, 1M Citric acid concentration, room temperature, 63 µm particle size, and a solid/liquid ratio of 1:10g/ ml. The experimental data are shown in Fig (3) as a relation of reaction time indicate that the leaching percent of U increased by about 22.0 to 83.0 % for U as the reaction time increased from 15 to 180 min. Increased stirring time of more than 180 minutes has a slight effect on the leaching efficiency of U. From the results, the reaction dissolution time was fixed at 180 min in all subsequent experiments [24].

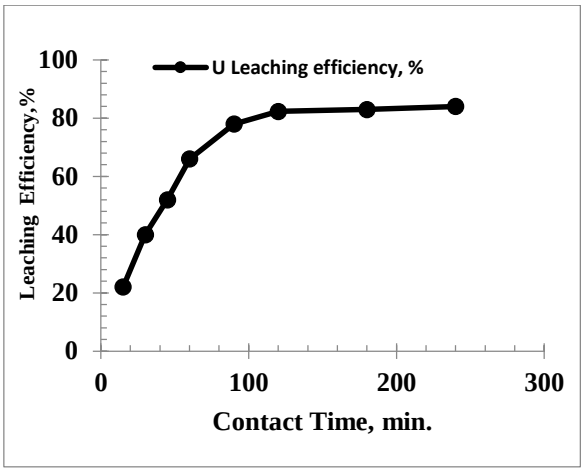

Fig. (3): Effect of Effect of reaction time on U dissolution efficiency, % temperature: 25±1°C; particle size: 63 µm; [Citric acid]: 1.0 M; S/L mass ratio: 1:10 g / ml; stirring speed: 600 rpm).

3.1.4. Effect of particle size

The effect of particle size on U leaching was investigated using six different particle sizes: 400 µm, 300 µm, 149 µm, 100 µm, 63 µm, and 32 µm. As the particle size of the working ore decreased from 400 to 63 µm, the U leaching efficiency increased from 18.0 to 83.0 %, as shown in Fig (4). This is due to the lowest particle size fraction having the maximum surface area; conversion rates are inversely related to the average initial diameter of the particles [25]. Increased particle size of more than 63 µm has a slight effect on the leaching efficiency of U. Hence the preferred particle size was 63 µm.

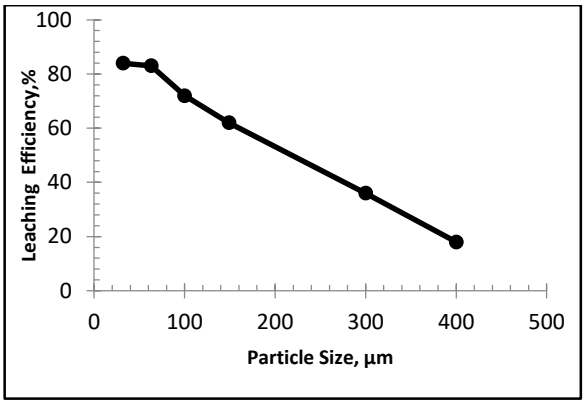

Fig. (4): Effect of particle size on U dissolution efficiency, % (room temperature; Citric acid: 1 M; stirring time: 120 min; S/L mass ratio: 1:10 g / mL stirring speed: 600 rpm).

3.1.5. Effect of solid / liquid ratio

At a reaction time of 120 min, a stirring speed of 600 rpm, an acid concentration of 1.0 M, room temperature, and a particle size of 63 µm, Figure (5) shows the effect of solid/liquid ratio on U dissolution. With an increase in the solid/liquid ratio from 1 to 20 g/ ml, the experimental results indicated a continuous increase in U from 18.0 to 84.00 %. This could be attributed to the decrease in the migration of uranium ions to the liquid medium as the bulk density of the solution increases. Increases in the solid/liquid ratio at more than 1:10 g/ml rarely affect leaching efficiency. As a result, for the other dissolution studies, 1:10 g/ml ore/ citric acid ratio is the optimum condition [26].

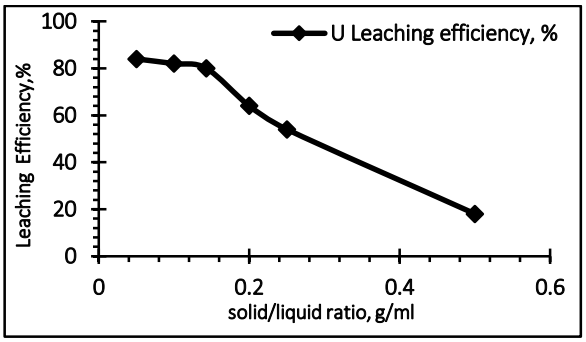

Fig. (5): Effect of solid/ liquid ratio on U dissolution efficiency, % (stirring speed: 600 rpm; particle size: 63 µm; [Citric acid]: 1.0 M; stirring time: 120 min; temperature: 60ºC.

3.1.6. Effect of temperature

The effect of reaction temperature on the dissolution process was studied at temperatures of 25, 30, 40, and 50 ºC with a reaction time of 120 minutes, a stirring speed of 600 rpm, a citric acid concentration of 1.0 M, a particle size of 63 µm, and a solid/liquid ratio of 1:10 g/ ml. As shown in Fig. (6), as the temperature of the working ore increased from 25 to 50ºC, the U leaching efficiency increased from 82.0 to 90.0 %. By increasing the reaction temperature from 25 to 50ºC, the dissolution efficiency of U was increased. As a result, the optimum temperature for the other factors experiments is 50ºC [27].

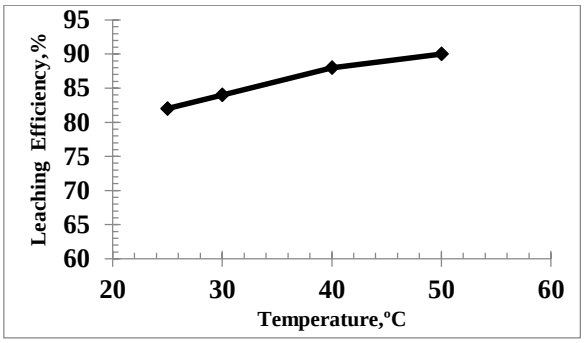

Fig. (6): Effect of reaction temperature on U dissolution efficiency, % (stirring speed: 600 rpm; particle size: 63 µm; S/L mass ratio: 1:10 g / ml; stirring time: 120 min; [Citric acid]: 1.0 M).

3.1.7. Preparation of pregnant leach liquor from contaminated soils

An extensive study on 5.0 kg of contaminated soils was treated using the preferred leaching conditions (1.0 M citric acid, agitation time 180 min, S/L ratio 1/10, grain size 63µm, stirring speed 600 rpm at ambient temperature) assayed 100 mg/L U. The pH was determined as 1.0 and was then re-adjusted by using 10 % NaOH solution to be introduced to the adsorption system. Batch stirring adsorption technique was applied in the present study. Natural zeolite (NZ) was used for uranium adsorption from leach liquor. Uranium adsorption from the pregnant citrate leach liquor had been studied in details using natural zeolite.

3.2. Optimization of uranium adsorption conditions

3.2.1.Effect of pH

Uranium adsorption is strongly dependent on pH of a solution because both degree of ionization (speciation) and the surface charge of NZ change as a function of pH. The effect of pH on adsorption efficiency of uranium from citrate solution with different pH (from 0.4 - 4.5) was investigated in **Fig. (7)**. The obtained results show that the adsorption efficiency was increased with increasing pH value and reached 70.0 % by increasing the pH of the solution to 2.5 which is measured as the preferred pH. The speciation distribution (degree of ionization) of uranium in citrate media was considered and characterized in **Fig. (8)**. The achieved results show that the complexes of UO_2^{2+} were the chief species at the pH range from 0- 4. Under almost alkaline and neutral pH conditions, a U-hydroxide complex begins to dominate the aqueous phase. In the range of pH 2.0

to 8.5, the $UO_2(Cit)^-$ and $UO_2(Cit)^{2-}$ becomes the main component of total concentration

whereas at pH 12, $UO_2(OH)_2.H_2O$ became the most species [28].

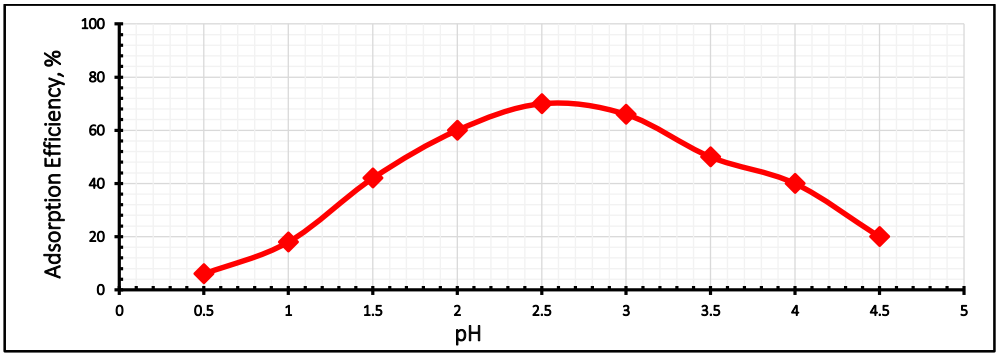

Fig. (7): Effect of pH on the adsorption of uranium

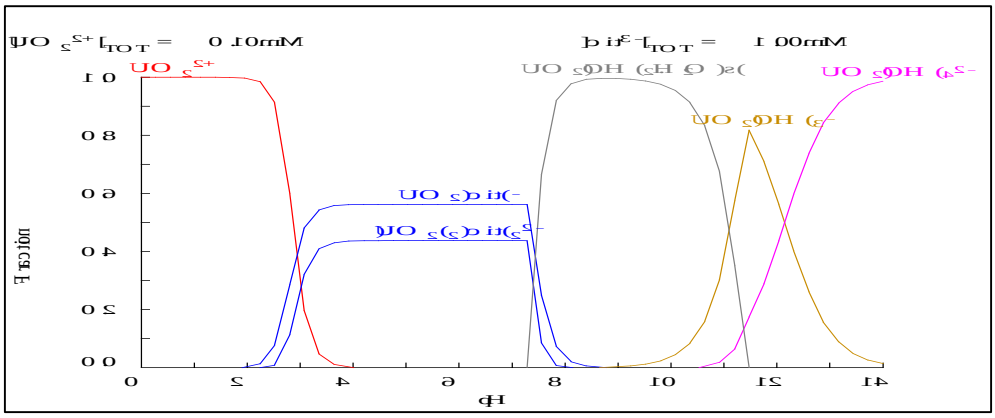

Fig. (8): Speciation of uranium (100 mg/L) as a function of pH in 0.1 M Citric acid using Medusa/Hydra program

3.2.2.Effect of contact time

The influence of contact time on the efficiency of uranium adsorption was investigated using 10 ml of nitrate solution evaluating 100 mg U/L was studied in the range of 5 to 240 minutes whereas the other conditions were kept at pH 2.5 and using 0.05 g NZ at room temperature. The results were summarized in **Fig. (9)** from the achieved results it is clear that the adsorption efficiency of uranium was increasingly increased as the contact time increased from 5 to 240 minutes, and the preferred adsorption efficiency (72.0%) was reached after 90 minutes. The equilibrium adsorption time was considered to be 120 minutes. Further increase in reaction contact time, the interval adsorption process has been the same. This may be associated with a decrease in the active sites of NZ and, moreover, with a decrease in the concentration of uranium in the solution [29, 30].

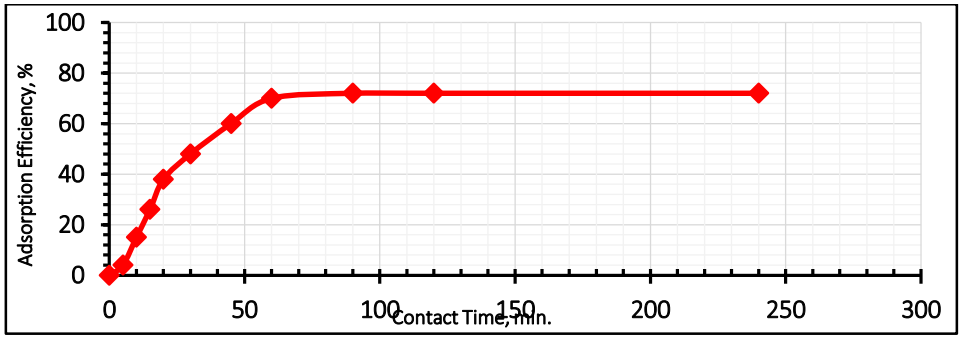

Fig. (9): Effect of contact time on uranium adsorption efficiency onto NZ

3.2.3.Effect of temperature

The temperature effect on uranium adsorption from synthetic nitrate solution was examined at various reaction temperatures ranging from 25 to 50ºC under the condition of a reaction time of 90 min, 10 mL of uranium with concentration 100 mg/L at solution pH 2.5 with 0.05g NZ. The results in **Figure (10)** indicate that the uranium adsorption decreased by the increase in temperature from 25 to 50ºC while the uranium adsorption decreases from about 61.6 to 50%. The most suitable adsorption temperature for the removal of uranium in citrate solution using NZ was obtained at 25 °C. Based on the obtained results, the room temperature represents the selected reaction temperature [31, 32].

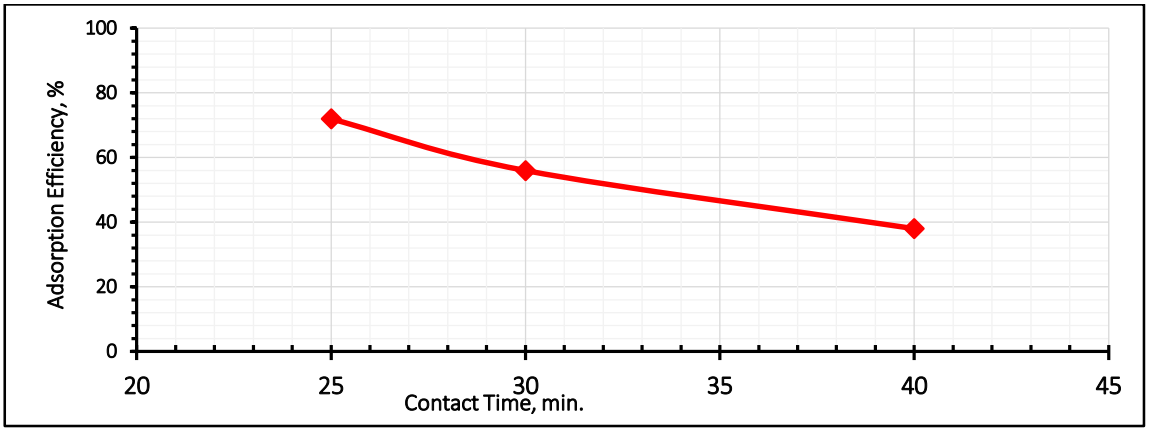

Fig. (10): Effect of temperature on uranium adsorption efficiency

3.2.4.Effect of NZ dosage

Under the condition that the NZ weight from 0.005 to 0.1 g, the uranium concentration is 100 mg/l and the pH is 2.5, for 120 min the effect of adsorbent dose on the uranium adsorption efficiency and uranium absorption rate was investigated.

As shown in **Fig. (11)** the experimental data was found to the adsorption efficiency of uranium improved sharply by increasing the adsorbent dose from 0.005 to 0.1 g. Additional increases in NZ concentration from 0.08 to 0.1 g was unable to produce important removal due to low uranium concentration in solution. This behaviour can be recognized as the improvement in the adsorption active sites and NZ surface area. Maximum adsorption efficiency of uranium removal value of 32.0% was attained at adsorbent dose of 0.05 g adsorbent in 10 ml citrate solution [33, 34].

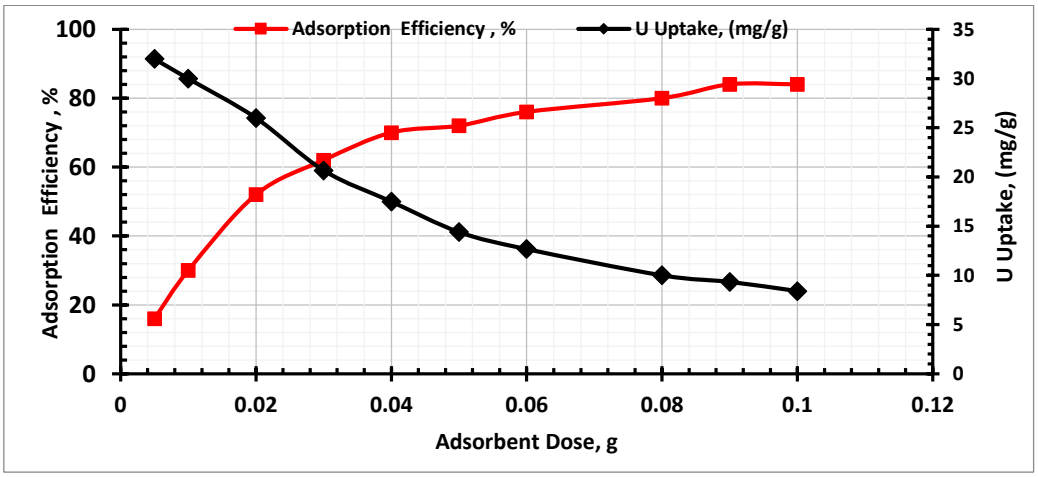

Fig. (11): Effect of NZ dose on adsorption of uranium

3.2.5. Effect of Initial Uranium

The uranium adsorption efficiency of NZ was examined as a function of the uranium initial concentration from 50 to 700 mg/L at a pH value of 2.5 for 90 min and using 0.05 g CHG at room temperature. As presented in **Fig. (12)**, it was found that the adsorption efficiency of uranium was decreased from 95.0 to 52.8% with increasing the uranium concentration from 50 to 700 mg/l whereas the uranium uptake was increased from 8.4 to 32.0 mg U/g. This decrease in the adsorption efficiency can be interpreted that the number of active sites on NZ is

decreased due to affinity of the uranium ions to bind with the active sites as a result of initial uranium concentration increase [35, 36]. Thus, the maximum saturation capacity of NZ was maintained at 32.0 mg U/g NZ.

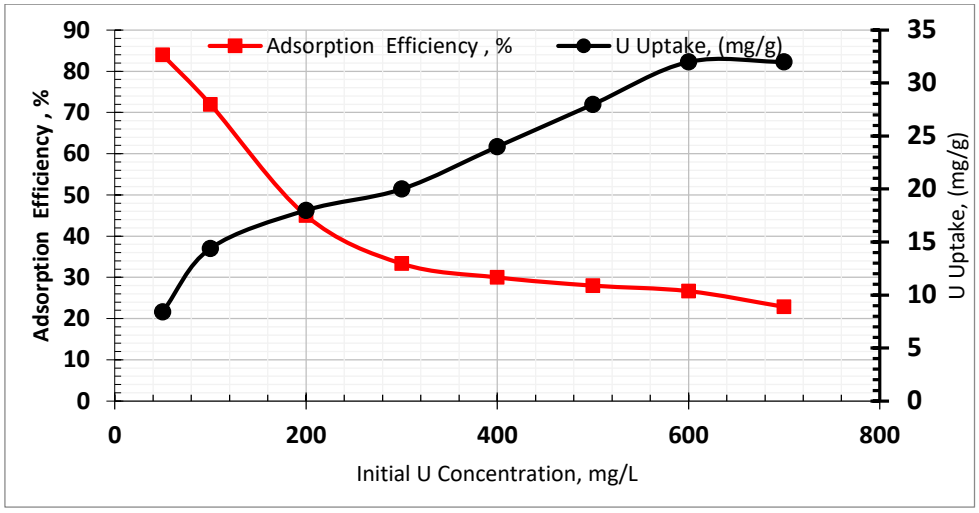

Fig. (12): Effect of initial uranium concentration on uranium adsorption efficiency onto NZ

3.3. Adsorption Kinetics and Mechanism

The kinetic models were used to investigate the mechanism of adsorption. The adsorption kinetics studies and mechanisms were employed as a function of temperatures (25 - 40 ºC) and estimated by pseudo-first-order (Lagergren equation) and pseudo-second-order models to describe the rate-controlling step of the adsorption interactions. The obtained results of batch experiments were evaluated using two models equations to evaluate the rate of the adsorption interactions [37, 38].

$$Log(q_e - q_t) = \text{Log}q_e - \left(\frac{K_1}{2.303}\right)t$$

Pseudo-first-order

Where q_t and q_e are the amounts of uranium adsorbed at certain time t (mg/g) and equilibrium (240 min.), respectively. Equilibrium adsorption capacity q_e (mg/g) values and rate constant K_1 (min^{-1}) of pseudo-first-order were obtained from the intercept and slope of the plot log (q_e–q_t) versus t for uranium adsorption at several temperatures as presented in **Figure (13 A)**. As summarized in **Table (1)**, the values of correlation coefficient (R^2) for the pseudo-first-order kinetic are ranged from 0.962 to 0.588. In addition to, the calculated maximum adsorption capacity (q_{ecal}) is far away from that is achieved experimentally (q_{eexp}). Pseudo first order mechanism data did not fit when applied on uranium adsorption by NZ [37, 38].

$$\frac{t}{q_t} = \frac{1}{K_2 q_e^{\,2}} + \left(\frac{1}{q_e}\right)t$$

Pseudo-second-order

K_2 (min^{-1}) refers to the pseudo-second-order rate constant and q_e (mg/g) equilibrium adsorption capacity values were obtained experimentally from the slope and intercept of plot t/q_t versus t as illustrated in **Fig. (13 B)**. The pseudo-second-order plot displays straight lines with good linearity with different temperatures. As shown in **Table (1)**, experimental equilibrium adsorption capacity (q_{eexp}) of uranium adsorption over NZ was 15.52, 12.0, and 8.31 mg/g at 25, 30 and 40 °C, respectively. Additionally, an extremely high correlation coefficient (R^2) was obtained ranged from 0.992 to 0.991 closer to unity for all concentrations at the four different temperatures. The kinetic model provides the best agreement between the calculated values of q_e and the experimental q_e data. The results suggest that the uranium adsorption mechanism on NZ followed the pseudo-second-order.

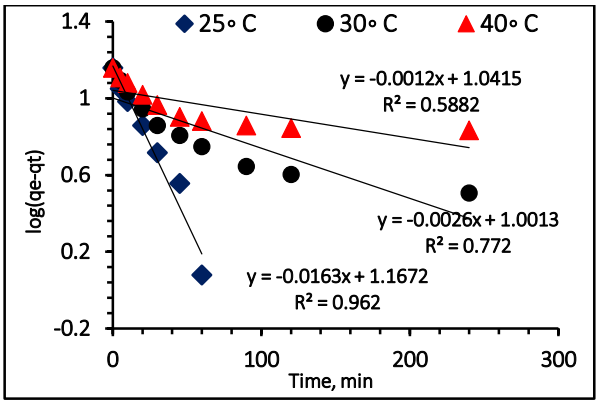

Fig. (13 A): Pseudo-first-order plot of uranium adsorption on NZ

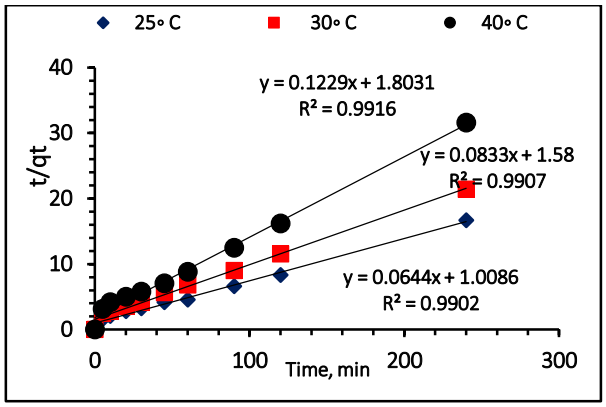

Fig. (13 B): Pseudo-second-order plot of uranium adsorption on NZ

Table (1): kinetic parameters for adsorption of uranium onto NZ adsorbent

Temp, °C	Lagergren pseudo first-order				Pseudo second-order			
	K_1(min $^{-1}$)	q_{ecal} (mg/ g)	q_{eexp} (mg/g)	R^2	K_2(min $^{-1}$)	q_{ecal}(mg/g)	q_{eexp} (mg/g)	R^2
25	0.033	14.4	21.34	0.962	0.0041	14.4	15.52	0.990
30	0.012	11.2	22.05	0.772	0.0043	11.2	12.00	0.990
40	0.007	7.6	22.89	0.588	0.0083	7.6	8.13	0.991

3.4. Adsorption Isotherms

Adsorption isotherms play an important role in determining the maximum adsorption capacity of NZ. The relationship between the adsorption capacity of uranium and its equilibrium concentration was investigated using several models in order to correlate the experimental data of the adsorption isotherms obtained through batch experiments. In general, the Langmuir and Freundlich isotherms are the most widely used isotherm models for NZ applications in aqueous solutions. The Langmuir and Freundlich model [39, 40] was used to measure equilibrium data. The isotherm of the Langmuir describes the adsorption of uranium ion to ligand sites (NZ) in a single layer on the NZ surface; the energy of adsorption is constant and has no interaction with the adsorbed species. In addition, there is no migration of uranium in the surface plane. The following equation of the linear form of the Langmuir isotherm was used[39, 40]: :

$$\frac{C_e}{q_e} = \frac{C_e}{q_{max}} + \frac{1}{K_L q_{max}}$$

q_{max} is the maximum adsorption capacity of saturated monolayer (mg/g), K_L is the Langmuir constant or equilibrium adsorption constant (L/mg), C_e (mg/L) represents the equilibrium concentration of uranium while q_e (mg/g) is the amount of uranium adsorbed at equilibrium per unit mass of NZ. q_{max} and K_L were estimated from the linear graph of C_e/q_e against C_e as presented in **Fig. (14).**

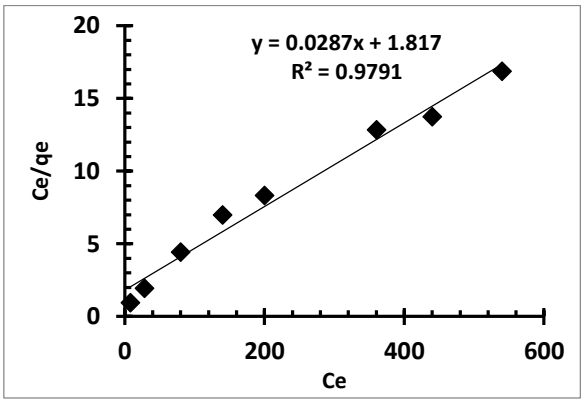

Fig. (14): Langmuir isotherm model of U (VI) adsorption onto NZ

On the other hand, the Freundlich isotherm model assumes that the energy of adsorption exponentially decreases as the adsorption active sites (NZ) are fully occupied. The Freundlich isotherm determines the adsorption which occurred on the heterogeneous surface and the interaction among the adsorbed molecules (multilayer adsorption). The Freundlich equation with linear form can be expressed as follows[39, 40]:

$$Logq_e = LogK_f + \frac{1}{n} LogC_e$$

where q_e represent the equilibrium adsorption capacity (mg/g), C_e represent the equilibrium concentration of uranium in solution (mg/L), KF is Freundlich constant which represent the adsorption capacity and n is Freundlich constant which represent adsorption intensity. K_F and n can be derived from the intercept and slope of the linear graph of log q_e against log C_e as illustrated in **Fig. (15)**. The Langmuir and Freundlich constants are represented in **Table (2).**

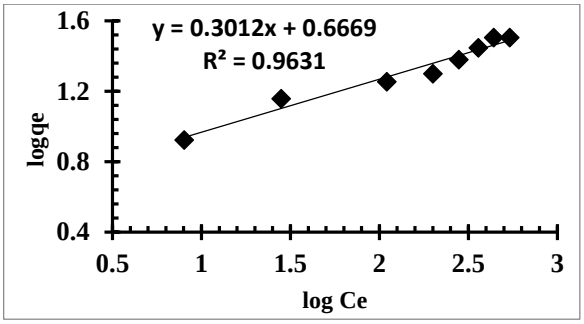

Fig. (15): Freundlich adsorption isotherm model of U (VI) adsorption on NZ

Table (2): Langmuir and Freundlich constants for uranium adsorption on NZ

Langmuir model parameters			Freundlich model parameters		
q_{max}	K_L	R^2	n	K_f	R^2
35.08	0.0124	0.979	3.104	4.126	0.963

From the obtained data of the equations of the Langmuir and Freundlich isotherms, it was found that the uranium adsorption on NZ correlates quite well (R^2 > 0.9) with the Langmuir equation compared to the Freundlich equation under the considered concentration range. In the Freundlich isotherm model, The **K_f** had a low value, and the **n** value indicated that the Freundlich isotherm was insufficient to describe the adsorption process of uranium into NZ. According to the Langmuir isotherm model, the maximum value of the correlation coefficient R^2 of the straight lines was near to the unity which displays a good linear relationship. In addition to the q_{max} and K_L calculated from the intercept and the slope of Langmuir plot were found to be 35.08 mg/g and 0.0124 L/mg respectively. It can be established that the employed adsorption system follows the Langmuir adsorption isotherm, which is sufficient to define the adsorption equilibrium of uranium on the NZ adsorbent.

3.5. Elution Experiments studies

The regeneration and reuse from the loaded NZ has been examined using the subsequent different eluent; CH_3COONa, NaOH, Na_2SO_4, HNO_3, H_2SO_4, Na_2CO_3, NaCl, and HCl. The uranium elution was performed using a batch technique at room temperature. The elution experiments studies were occurred by shaking 0.1 g loaded NZ and 10 mL of 1 molar for eluting media for 1 hour at 250 rpm. The obtained result of uranium desorption from the NZ using different solutions was evaluated systematically and shown in **Table (3)**. From the results obtained, it is clearly obvious that a promising result was achieved with HCl among the eluents used in this study, where (HNO_3, H_2SO_4, and HCl) wash of metal-loaded NZ released 72.9 %, 84.6%, and 93.8%, respectively, while the others eluent give low elution efficiency.

Table (3): Uranium recovery from loaded NZ using different solutions

Eluent Type, 1.0 molar	Efficiency,%
H_2SO_4	84.6
HCl	93.8
HNO_3	72.9
CH_3COONa	28.5
Na_2SO_4	30.7
Na_2CO_3	42.8
NaOH	38.2

3.6. Reusability Study Experiments

The advantage of using a NZ is the ability to regenerate after reaching capacity. For this purpose, reusability is the most significant feature of an advanced adsorbent. For economy and originality, NZ must be reusable, and because of the reversible adsorption process, regeneration of the absorbent is possible [41]. Hence, the reusability of the NZ adsorbent, the cyclic adsorption-desorption study was carried out. From the data in **Table (4)**, it was found that the adsorption efficiency of the NZ decreases slightly with each cycle. Even after 5 cycles, the adsorbent still shows high adsorption efficiency. The results obtained confirmed the possibility of using NZ adsorbents to adsorb uranium from citrate solutions.

Table (4): Adsorption-desorption cycle for recovery of uranium with NZ

No. of cycle	Sorption Efficiency,%	Desorption Efficiency,%
1	83.8	74.5
2	62.3	55.8
3	38.9	32.9
4	22.9	15.9
5	5.7	3.6

3.7. Characterization of the natural zeolite

3.7.1. XRD analysis

The XRD patterns of the natural zeolite confirming the mineralogy by using X ray Diffraction analysis which was applied to detect the crystallinity of the the natural zeolite The NZ powder showed The sharp

feature peaks around 2θ = 7.1°, 20.3°, 38.5°,58.4 and 65.9° were attributed to the crystalline structure of the NZ powder as shown in Fig. 16.

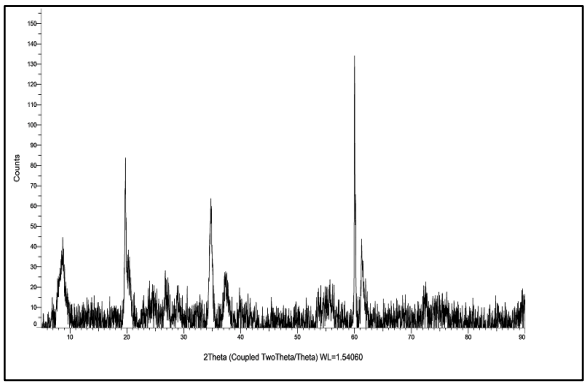

Fig. (16): XRD patterns of NZ before uranium adsorption

3.7.2. Energy dispersive X-ray (EDX) spectroscopy and Surface Morphology Studies of NZ

EDX and analysis of **NZ** was accomplished to determine the chemical composition (elemental analysis) before and after loading the uranium ion. The natural zeolites before loading was analyzed by EDX consist of mainly Si, Na, and Al as revealed in **Fig. (17A)**. NZ after adsorption of uranium ions was characterized by EDX showed the occurrence of Na, Si, Fe, K, and U. The results confirmed the uranium adsorption by NZ as presented in **Fig. (17B).**

The SEM images in **Figs. (17A, B)** Display the configuration of the NZ before and after the adsorption of uranium. The surface morphology of the NZ contains a porous structure which allows the uranium molecules to diffuse into hydrogel, causing swelling. Generally this means that the organized NZ has a porous structure that supports to the adsorption of uranium from aqueous solutions. Then, the uranium solution was spread in the NZ and well spread on the surface of the NZ.

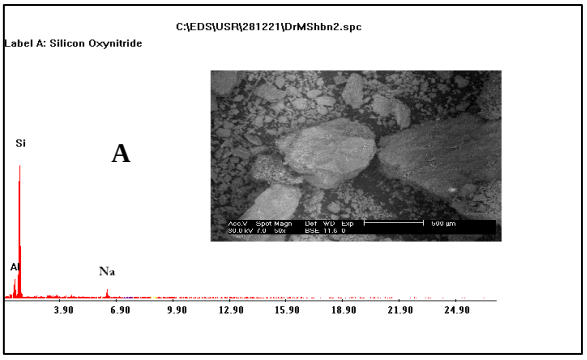

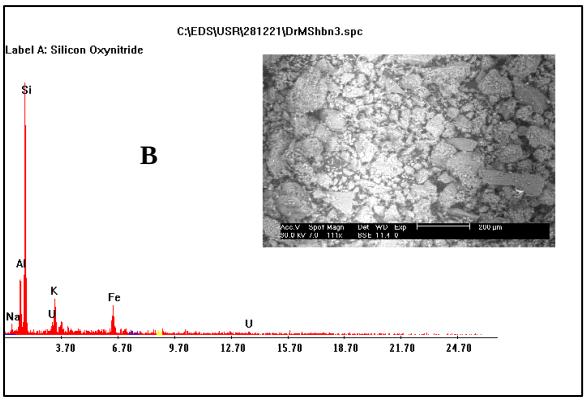

Figs. (17): EDX spectrum and SEM images of NZ (A) before uranium adsorption and (B) after adsorption of uranium

3.8. Characterization of the soil

3.8.1. XRD analysis

The XRD patterns of the soil confirming the mineralogy by using X ray Diffraction analysis which was applied to detect the crystallinity of the soil. The soil powder showed the sharp feature peaks around 2θ = 28.1°, 32.3°, 40.5°, and 55.4 were attributed to the crystalline structure of the soil powder as shown in Fig. 18.

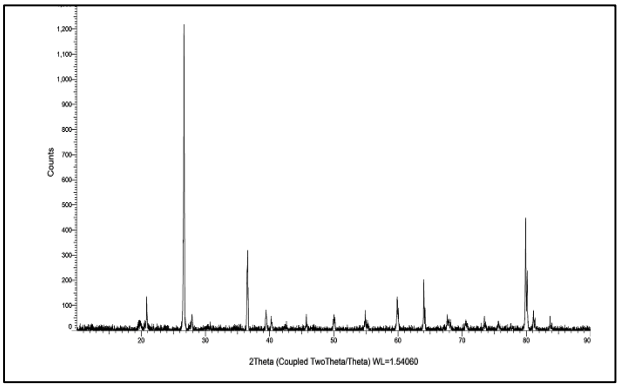

Fig. (18): XRD patterns of soil before uranium adsorption

3.8.2. Energy dispersive X-ray (EDX) spectroscopy and Surface Morphology Studies of soil

EDX and analysis of **soil** was accomplished to determine the chemical composition (elemental analysis) before and after loading the uranium ion. The natural zeolites before loading was analyzed by EDX consist of mainly Mg, Si, K, Fe and Al as revealed in **Fig. (19A)**. **Soil** after adsorption of uranium ions was characterized by EDX showed the occurrence of Mg, Si, Fe, K, Al and U. The results confirmed the uranium adsorption by soil as presented in **Fig. (19B).**

The SEM images in **Figs. (19A, B)** Display the configuration of the before and after the adsorption of uranium. The surface morphology of the soil contains

a porous structure which allows the uranium molecules to diffuse into soil, causing swelling. Generally this means that the organized soil has a porous structure that supports to the adsorption of uranium from aqueous solutions. Then, the uranium solution was spread in the soil and well spread on the surface of the soil.

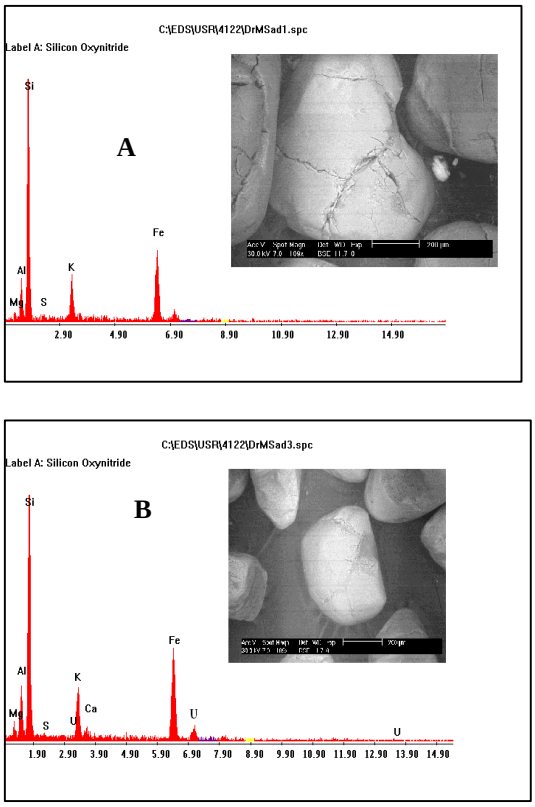

Figs (19): EDX spectrum and SEM images of soil (A) before uranium adsorption and (B) after adsorption of uranium

4. Conclusion

In this study, the leaching of u from contaminated soil using citric acid solution has been investigated. The results showed that the reaction rate increases with time, hydrogen ion [h+] concentration, liquid/ solid mass ratio, while leaching temperature and stirring speed have a slightly effect on the leaching rate. Natural zeolite was characterized by x-ray diffraction (xrd), and scanning electron microscope (sem). Nz has been tested for uranium adsorption from citrate solution. The adsorption kinetics mechanism obeys a pseudo-second-order rate equation and the adsorption process was well fitted with the langmuir isotherm model with a maximum monolayer adsorption capacity of qmax = 35.0 mg u/g nz at ph 2.5 for 120 minutes' contact time at ambient temperature. The uranium desorption from the nz by using 1 m hcl achieved 93.8% desorption efficiency.

5. References

1) Donia AM, Atia AA, Moussa MM, Sherif AM, Magied MO (2009) Hydrometallurgy 95:183.
2) Ganesh R, Robinson KG, Chu LL, Kucsmas D, Reed GD (1999) Water Res 33:3447
3) Kryvoruchko AP, Yurlova LY, Atamanenko ID, Kornilovich BY (2004) Desalination 162:229
4) Mellah A, Chegrouche S, Barkat M (2006) J Colloid Interface Sci 296:434
5) Kadous A, Didi M, Villemin D (2009) J Radioanal Nucl Chem 280:157
6) Sodayea H, Nisanb S, Poletikoc C, Prabhakara S, Tewaria PK (2009) Desalination 235:9
7) Gupta VK, Rastogi A (2008) Colloids Surf B 64:170
8) Panuccio MR, Crea F, Sorgona` A, Cacco G (2008) J Environ Manag 88:890
9) Kundu S, Gupta AK (2005) J Colloid Interf Sci 290:52
10) Kocaoba S, Orhan Y, Akyu¨z T (2007) Desalination 214:1
11) Peric J, Trgo M, Medvidovic NV (2004) Water Res 38:1893
12) Babel S, Kurniawan TA (2003) J Hazard Mater 97:219
13) Rynskyy M, Buszewski B, Terzyk AP, Namies´nik J (2006) J Colloid Interface Sci 304:21
14) Loizidou M, Townsend RP (1987) Zeolites 7:153
15) Leppert D (1990) J Min Eng 42:604
16) Kilincarslan A, Akyil S (2005) J Radioanal Nucl Chem 264:541
17) Misaelides P, Godelitsas A, Filippidis A, Charistos D, Anousi I (1995) Sci Total Environ 173/174: 23
18) Krestou A, Xenidis A, Panias D (2003) Miner Eng 16:1363
19) Akyil S, Aslani M A A, Aytas X S (1998) J Alloys Compd 271/273: 769
20) Ames LL, McGarrah JE, Becky AW (1983) Clay Clay Miner 31(5):321
21) Z. Marczenko Z, and M. Balcerzak, Separation, preconcentration and spectrophotometry in inorganic analysis. (Amsterdam: Elsevier Science B.V., 2000) p 521
22) El Sayed A. Haggag, Mahmoud S. Khalafalla & Ahmed M. Masoud (2021) Leaching kinetics of uranium, rare earth elements and copper using tartaric acid from El Allouga ore material, Southwestern Sinai, Egypt, International Journal of Environmental Analytical Chemistry, DOI: 10.1080/03067319.2021.1991334
23) Khawassek Y. M.; Eliwa A.A.; Haggag E. A.; Saad Mohamed A.; Omar S. A. (2016). Kinetics Leaching Process of Uranium Ions from El-Erediya Rock by Sulfuric Acid Solution. International Journal of Nuclear Energy Science and Engineering, 6; 48-35. DOI: 10.14355/ijnese.2016.06.004
24) Moussa M. A.; Daher A. M.; S Omar. A.; Y Khawassek. M.; Haggag E. A.; Gawad E.A.

(2014) Kinetics of leaching process of Uranium from EL-Missikat shear zone Eastern Desert, EGYPT .J. of Basic and Environmental Sciences, 1; 65-75.

25) Khawassek Y. M.; Gawad E. A.; Haggag E. A.; Eliwa A. A. (2015) Kinetics of Leaching Process of REE from El-Missikat Shear Zone Eastern Desert, EGYPT. J. of Chemical Technology, 10(6); 295-306.
26) Zafar Z.I.; Ashraf M. (2007) Selective leaching kinetics of calcareous phosphate rock in lactic acid. Chemical Engineering Journal, 131; 41-48. https://doi.org/10.1016/j.cej.2006.12.002
27) M. Gharabaghi, M. Noaparast, M. Irannajad, (2009), Selective leaching kinetics of low-grade calcareous phosphate ore in acetic acid, Hydrometallurgy 95: 341–345.
28) I. Puigdomenech (2006) HYDRA (Hydrochemical Equilibrium-Constant Database) and MEDUSA (Make Equilibrium Diagrams Using Sophisticated Algorithms) Programs. Royal Institute of Technology, Stockholm. Royal Institute of Technology, Sweden. http://www kemi kth se/medusa
29) Haggag, El Sayed A., Abdelsamad, Ahmed A., Masod, Mohamed, B., Mohamed, Mostafa M. Ebiad, Mohamed A., "Kinetic studies on the adsorption of uranium on a mesoporous impregnated activated carbon", Egyptian Journal of Chemistry, Vol.64, No.3 pp.1371-1385 (2021).DOI:10.2608/EJCHEM.2020.50611.3039
30) El-Sheikh, A. S., Haggag, E. A., and Abd El-Rahman, N. R. "Adsorption of Uranium from Sulfate Medium Using a Synthetic Polymer; Kinetic Characteristics", Radiochemistry, 2020, Vol. 62, No. 4, pp. 499–510. doi.org 10.1134/S1066362220040074
31) Dacrory, Sawsan, Haggag, El Sayed A., Masoud, Ahmed, M., Abdo, Shaimaa, M., Eliwa, Ahmed, A. and Kamel, Samir., "Innovative Synthesis of Modified Cellulose Derivative as a Uranium Adsorbent from Carbonate Solutions of Radioactive Deposits, Journal of Cellulose, 29 May 2020. https://doi.org/10.1007/s10570-020-03272-w
32) Mahmoud, M. A., Gawad, E. A., Hamoda, E.A., and Haggag E. A., "Kinetics and Thermodynamic of Fe (III) Adsorption Type onto Activated Carbon from Biomass: Kinetics and Thermodynamics Studies", J. of Environmental Science, 11(4), (128-136), (2015). ISSN : 0974 - 7451
33) Abdel-Samad, A. A., Abdel Aal, M. M., Haggag, E. A., Yosef, W. M., Synthesis and Characterization of Functionalized activated Carbon for Removal of Uranium and Iron from Phosphoric Acid, Journal of Basic and Environmental Sciences, 7 (2020) 140-153. Online: 2356-6388
34) Haggag, El Sayed A., Abdelsamad, Ahmed A., Masoud, Ahmed M. "Potentiality of Uranium Extraction from Acidic Leach Liquor by Polyacrylamide-Acrylic Acid Titanium Silicate Composite Adsorbent", International Journal of Environmental Analytical Chemistry, July, (2019), doi.org/10.1080/03067319.2019.1636037.
35) Khawassek, Y.M., Eliwa, A.A., Haggag, E. A. Omar S. A. and Mohamed S. A. Adsorption of rare earth elements by strong acid cation exchange resin thermodynamics, characteristics and kinetics. SN Appl. Sci. 1, 51 (2019). https://doi.org/10.1007/s42452-018-0051-6
36) Khawassek, Y. M Eliwa, A. A. Haggag, E. A. Mohamed S. A. and S. A. Omar "Equilibrium, Kinetic and Thermodynamics of Uranium Adsorption by Ambersep 400 SO4 Resin", Arab Journal of Nuclear Sciences and Applications, Vol 50, 4, (100-112), (2017). Web site: esnsa-eg.com.
37) Lagergren, S. (1898) Zur theorie der sogenannten adsorption geloster stoffe, Kungliga Svenska Vetenskapsakademiens. Handlingar, 24, 1-39.
38) Ho, Y.S. and McKay, G. (1999) Pseudo-Second Order Model for Sorption Processes. Process Biochemistry, 34, 451-465.https://doi.org/10.1016/S0032-9592(98)00112-5
39) Lagergren, S. (1898) Zur theorie der sogenannten adsorption geloster stoffe, Kungliga Svenska Vetenskapsakademiens. Handlingar, 24, 1-39.
40) Ho, Y.S. and McKay, G. (1999) Pseudo-Second Order Model for Sorption Processes. Process Biochemistry, 34, 451-465. https://doi.org/10.1016/S0032-9592(98)00112-5
41) Haggag, E. A., (2021) Cellulose hydrogel for enhanced uranium (VI) capture from nitrate medium: preparation, characterisation and adsorption optimisation, International Journal of Environmental Analytical Chemistry, DOI:10.1080/03067319.2021.2005791